

Optimisation of Low Temperature Combustion Technology, for Future Drive Cycles, using a Factorial Design of Experiments

A.S. van Niekerk, P.J. Kay, B. Drew, N. Larsen
University of the West of England

Copyright © 2019 SAE Japan and Copyright © 2019 SAE International

ABSTRACT

Automotive manufacturers are facing increased pressure to meet more stringent emissions legislation and new legislative driving cycles. One technology that has the potential to meet future legislation is Low Temperature Combustion (LTC), which has the potential to significantly reduce NO_x over conventional diesel combustion. Most studies reported in the literature evaluating this technology only change 'one-factor-at-a-time' at steady state conditions. This paper addresses these issues and presents a methodology utilising DoE analysis to optimise a validated multi-fidelity engine simulation for LTC over a transient cycle (WLTP) which makes the results more applicable to real world driving conditions.

A validated simulation for a 2.4-litre compression ignition engine was developed in Ricardo WAVE. To increase the fidelity of the model, empirical data such as 3D scans of the inlet geometry were included. The simulation was validated against experimental engine emissions and performance data. A characterization study using a full factorial DoE was performed on the whole engine simulation to minimise vehicle emissions using LTC. The vehicle simulation was tested against the WLTP and the response of the emissions for different levels of exhaust gas recirculation (EGR), pilot start of injection (SOI) and main SOI timings and pilot injection duration were recorded.

The results of the optimization showed that over the WLTP the NO_x emissions decreased by approximately 85 % with an EGR of 47.5 %, retarding the pilot SOI and main SOI maps with 1 CAD compared to the default maps and increasing the pilot injection duration by 200 microseconds. NO_x emissions were reduced by approximately 18 % with the use of 12 % EGR without exceeding the Euro 4 CO emissions limit. Further increase in EGR percentage significantly increased the CO emissions.

INTRODUCTION

The European Union (EU) has implemented successive emission standards to reduce the environmental impact of road transport and to help the transition towards a low carbon economy. These measures include a limit on CO₂ emissions as well as a separate Euro 6 legislation, which enforces limitations on harmful gasses in vehicle exhaust [1].

Viable after-treatment systems are available to meet the new emission limits, but higher costs, durability issues, fuel economy penalties and ever-increasing space requirements limit the widespread adoption of the devices. As a result, improvements to in-cylinder strategies to further reduce the engine-out emissions to decrease the burden put on after treatment systems, are of great interest [2]. Low temperature combustion (LTC) is a promising combustion concept that can successfully reduce in-cylinder emissions resulting in the significant reduction in after-treatment dependencies [3]. LTC is a term used to refer to combustion concepts where the overall goal is to achieve a reduction in peak combustion temperature. The reduction of peak combustion temperatures can be achieved by the use of early fuel injections or with the use of exhaust gas recirculation (EGR) [3, 4].

LTC technologies can have contrasting effects on cylinder temperature and air-fuel mixture. Carlucci et al. [5] found that advancing the pilot injection timing results in a trade-off between higher cylinder temperatures, which increases NO formation, and reduction of the main injection's ignition delay, which causes a decrease in premixed combustion as well as NO_x formation; resulting in lower NO_x overall. Also, the use of EGR increases the ignition delay of the main injection which promotes premixed combustion, but lowers the combustion temperature due to the increase in inert gasses in the inlet charge [6]. Table 1 summarises the effects that LTC technologies have on combustion temperature, and subsequently NO_x, and charge homogeneity. The "+" sign indicates an increase in value and the "-" sign indicates a decrease in value. In order to use LTC effectively, it is necessary

to optimise the use of different LTC techniques in a compression ignition engine to achieve emission reductions.

Current literature on LTC only focuses on evaluating one or two LTC techniques at a time, as summarised in Table 2. All the tests were conducted at steady-state engine operation which limits their value in accurately representing the on-road behaviour of the engines.

Table 1. Effect of different LTC strategies on combustion temperature and air-fuel mixture [5-13].

LTC strategy	Combustion Temperature	Charge Homogeneity
Increase pilot injection duration	+	+
Advance pilot injection SOI	+	+
Advance main injection SOI	-	-
Increase EGR percentage	-	+

Table 2. Scope of available literature on LTC technologies. PI is pilot injection and MI is main injection.

Output	PI	MI	EGR	Drive cycle
Engine performance [5,8]	X	X		Steady-state
Emissions [4,11,14]			X	Steady-state
Emissions [9]	X	X	X	Steady-state
Emissions [15]	X		X	Steady-state

Additionally, with compression ignition engines becoming more technically complex due to the restrictive emissions legislation, simulation has become a powerful tool in initial design and optimization. A method using a Design of Experiments (DoE) analysis on a validated simulation is presented. The use of non-linear techniques like DoE is suitable to explore the interaction effects of engine parameters and its combined effect on engine emissions. DoE is the most cost effective and economical technique to evaluate the individual effects and combined effects of the engine responses on the emissions. Simulation can also assist in the system development of new hardware when legislation requirements are changed. New drive cycles have introduced changes to the validation cycle with different velocity profiles and increased testing time, which ultimately covers a wider range of the engine's operating map. These changes need to be considered during optimization of the vehicle system and simulations need to be adaptable to these changes [16].

This paper investigates emission reduction with the use of an engine simulation to optimise LTC techniques in a compression ignition engine while being tested over the WLTP drive cycle. Engine parameters that are considered are the pilot injection and main injection start of injection (SOI) timings, pilot injection duration and the EGR percentage. DoE will be used to characterize the response of the

compression ignition engine and determine the parameters that significantly contribute to emission reduction. The statistical tool can be used to determine the operating parameters that result in the largest reduction in engine emissions over a given drive cycle. DoE allows for the investigation of multiple factors and their effect on engine performance and emissions. The levels of the factors are changed simultaneously, rather than one at a time. This contributes to a cost and time saving [17, 18]. The use of DoE is appropriate as other studies have used it successfully to investigate the effects between injection timing, injection pressure and nozzle tip protrusion on emission characteristics [19], to analyse the role of the injection system parameters on engine emissions, noise and fuel consumption [20] and to determine the optimum engine design and operating parameters [21].

The aim of this study is to add to the field by demonstrating the ability to reduce the cost of evaluating emission reduction technologies using high fidelity simulations and a DoE approach.

SIMULATION SETUP

The following sections discuss the setup of the engine simulation as well as the DoE method used to determine the path of greatest emission reduction.

ENGINE SIMULATION SETUP

The reduction of engine emissions by using LTC techniques were investigated with the use of a co-simulation between a one-dimensional engine simulation, Ricardo WAVE and a system-based simulation package, Ricardo IGNITE, to generate engine emissions data. Minitab, a statistical software package, was used for the DoE set-up and calculations. The co-simulation was set up improving upon the validated simulation of a 2.4 litre Euro 4 compression ignition engine used in previous published work [22]. Improvements include:

- Addition of empirical valve flow characteristics.
- Improved start of combustion calculations correlated to experimental data.
- Accurate piston crown and inlet runner dimensions derived from a 3D scanning technique.
- Increased controller accuracy to minimize error when following the selected drive cycle.

Although the research in this paper was conducted on a Euro 4 engine, which was manufactured in 2008, this research is still highly relevant to the current UK fleet. According to the Department for Transport's statistics [23] approximately 36 % of the current diesel fleet, of this vehicle type (light commercial vehicles) is Euro 4 vehicles. Additionally the conclusions for this paper are qualitatively relevant to more modern Euro 5 and Euro 6 compression ignition engines [24-26].

The simulation was validated, in terms of NO_x, CO and in-cylinder pressure, against steady state results from the engine. Details of the improved combustion and

emission models are available in the Appendix. The characteristics of the engine as well as the vehicle that were simulated over the WLTP are listed in Table 3 and Table 4. An after treatment system was not added to the simulation of the engine, as the emphasis is on reducing the emission from the combustion process. The stringent emission limits implemented by the EU are difficult to meet solely with the use of after treatment systems. The cost of adding complex after treatment systems also contributes to increased cost to the consumer. Scope to reduce emissions in-cylinder with the use of LTC poses benefits to cost reduction and decreased complexity in after treatment design [3, 11, 27].

Table 3. Specifications of the engine used in the one-dimensional engine simulation.

Displaced volume	2402 cc
Stroke	94.6 mm
Bore	89.9 mm
Connecting Rod	106 mm
Compression ratio	17.5:1
Number of Valves	16
Number of cylinders	4

Table 4. Specifications of the vehicle used to simulate engine emissions over the WLTP.

Vehicle mass	3500 kg
Rolling resistance coefficient	0.01125
Wheel radius	0.33 m
Final drive ratio	3.73
Frontal area	5.6 m ²
Drag coefficient	0.445

SIMULATION DESIGN SETUP

A 2⁴ factorial experimental design was used for the evaluation of engine emissions. Engine emission responses that were considered are CO emissions and NO_x emissions. Particulate Matter (PM) was not considered since the modelling of PM formation is complex [28] and not modelled in the software.

In order to determine the best overall reduction in engine emissions, values for the engine parameters after each simulated factorial design needs to be determined through optimization. Available optimization techniques include overlaying the response contour plots, constrained optimization and the desirability approach. Among them, the desirability approach was found to have benefits like simplicity, availability in the statistical software being used and has the flexibility to weigh and prioritise individual responses [29]. In the present work, the desirability approach was used for the optimization of the engine parameters for the simulated properties of the engine response (CO emissions and NO_x emissions). The software transforms each response to a dimensionless desirability value d . The value ranges from $d=0$, which indicates that the response is unacceptable, to $d=1$ which shows that the response is more

desirable. The goal of this study was to minimise all engine emissions and the desirability of each of the responses was calculated using [17]:

$$d_i(\hat{Y}_i) = \begin{cases} 1.0 & \text{if } \hat{Y}_i(x) < T_i \\ \left(\frac{\hat{Y}_i(x) - U_i}{T_i - U_i} \right) & \text{if } T_i \leq \hat{Y}_i(x) \leq U_i \\ 0 & \text{if } \hat{Y}_i(x) > U_i \end{cases} \quad (1)$$

where $d_i(\hat{Y}_i)$ is the desirability function of response $\hat{Y}_i(x)$. T_i and U_i are the target and upper values respectively that are desired for response $\hat{Y}_i(x)$. For minimising the response, T_i will denote a small enough value for the response. The individual desirability functions are combined using the geometric mean, which gives the overall desirability:

$$D = (d_1(Y_1) \times d_2(Y_2))^{0.5} \quad (2)$$

It is noticeable that if any response $d_i(\hat{Y}_i)$ is completely undesirable, $d_i(\hat{Y}_i) = 0$, then the overall desirability is zero.

The first factorial design started at the values listed in Table 5 relative to the default ECU maps. The initial values chosen for the parameters are based on available literature [4,5,9]. Default ECU maps for injection SOI are expressed in degrees after top dead center (aTDC) and the default map for injection duration is expressed in microseconds. The map values were changed as per the low and high levels of Table 5. At low engine speed values, the pilot injection SOI for the default ECU maps are approximately 20 CAD earlier than the main injection SOI. This decreases to approximately 14 CAD at high engine speed values. EGR operating maps were generated for each factorial design test point based on the values chosen from the desirability function.

Table 5. Independent variables and their levels for the first factorial design.

Independent variables	Variable levels		
	Low	High	Δ
EGR (%)	0	10	10
Pilot injection SOI (CAD)	-1	1	2
Pilot injection duration (μ s)	-100	100	200
Main injection SOI (CAD)	-1	1	2

Examples of the maps used can be seen in Figure 1 (10 % maximum EGR) and Figure 2 (45 % maximum EGR). The maximum EGR generated is always at approximately 10 % throttle position and 2500 rpm.

Additional factorial designs were performed in the direction indicated by the engine parameters that resulted in an optimum overall desirability factor. For engine parameters where the best combination is at the corner of a factorial plot, the next factorial design will share that corner with the previous factorial design and the difference in variable levels for the variables considered, will be increased by 50 %. For engine

parameters where the optimum variable level is at the side of the factorial plot, only that variable's difference in levels will be increased by 50 %. This can be seen graphically in Figure 3.

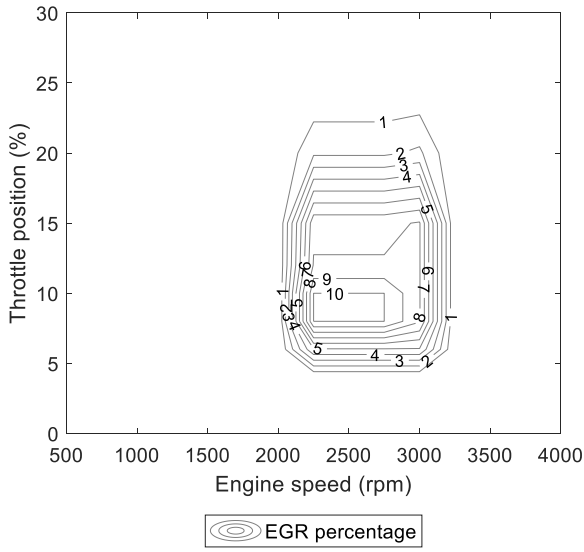


Figure 1. EGR operating map for a maximum EGR value of 10 %.

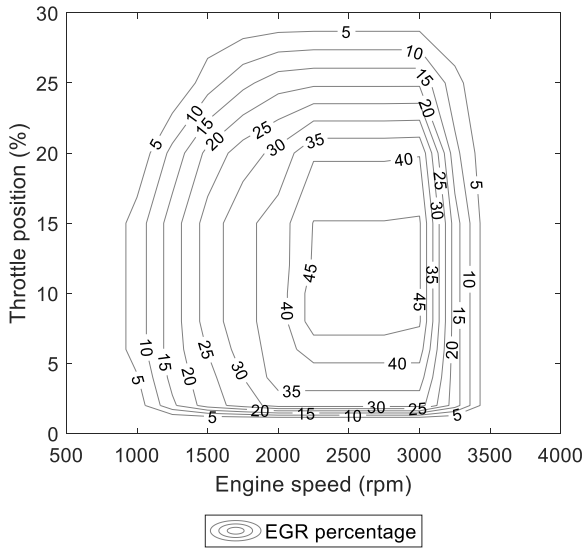


Figure 2. EGR operating map for a maximum EGR value of 45 %.

The selection process for the low and high values for the next factorial design can also be expressed by:

$$L_{i+1} = \begin{cases} H_i, & \max(D_i) = \text{True} \\ L_i, & \max(D_i) \neq \text{True} \end{cases} \quad (3)$$

and

$$H_{i+1} = \begin{cases} 1.5\Delta_i + H_i, & \max(D_i) = \text{True} \\ H_i, & \max(D_i) \neq \text{True} \end{cases} \quad (4)$$

where L and H indicate the low and high variables for a given factorial design and the operator i indicates the current factorial design under consideration.

Figure 3 shows a 2^2 factorial surface plot for EGR percentage and crank angle degrees added to the pilot injection SOI ECU map. The first factorial design as listed in Table 5, are shown graphically with the use of the box numbered 1. If significant emission reduction is identified for an EGR percentage of 10 % and a pilot injection SOI retarding of 1 CAD, then the second factorial design will investigate an area of EGR percentage between 10 % and 25 % and a pilot injection SOI retarding of between 1 and 4 CAD. If for the second factorial design an EGR percentage of 25 % and a pilot injection SOI retarding of approximately 3 CAD resulted in the most emissions reduction, then the third factorial design will investigate an area of EGR percentage between 25 % and 47.5 % and a pilot injection SOI retarding of between 1 and 4 CAD. The method will be used until an optimum in engine emission reduction through LTC is found.

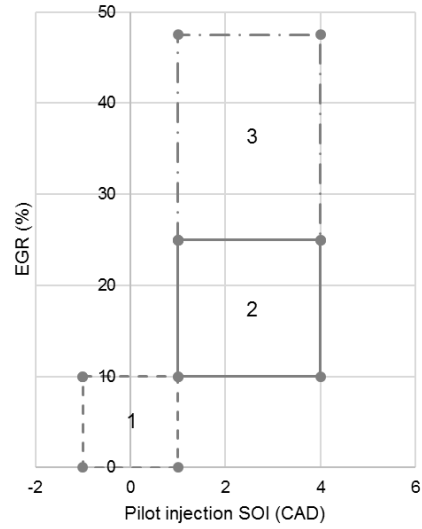


Figure 3. Example of the possible path for engine parameters after three factorial design iterations.

RESULTS AND DISCUSSION

The paper investigated the characterization and optimization of an engine's emissions response to LTC techniques when simulated over the WLTP legislative drive cycle. Engine parameters included pilot injection SOI, main injection SOI, pilot injection duration and EGR percentage and the engine response included CO emissions and NO_x emissions.

FIRST FACTORIAL DESIGN

Main effect plots are shown in Figure 4 and Figure 5 for CO emissions and NO_x emissions. Each line graph in Figure 4 and Figure 5 represent the change in emissions when the engine parameters are changed from the low to high values as seen in Table 5. The higher the gradient of the line, the more significant effect the engine parameter has on the engine response. Figure 4 shows that EGR percentage has the most significant effect on CO emissions, followed by the main injection SOI. Pilot injection SOI and pilot injection duration have comparatively little effect on the CO emissions in the engine's exhaust.

Figure 5 shows that EGR has the most significant effect on NO_x emissions, followed by pilot injection SOI and pilot injection duration. The main injection SOI has comparatively little effect on the NO_x emissions in the engine's exhaust.

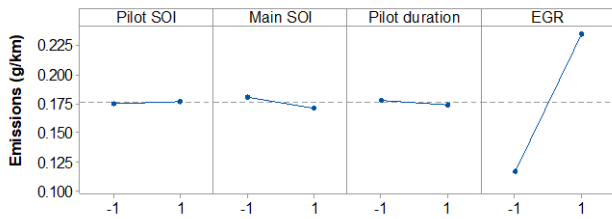


Figure 4. Variation of CO emissions against high and low levels for each of the main effects, for the first factorial design.

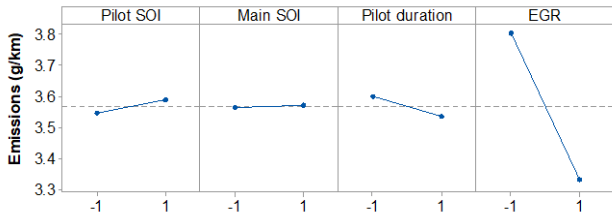


Figure 5. Variation of NO_x emissions against high and low levels for each of the main effects, for the first factorial design.

Figure 6 shows the desirability plot for the first factorial design. The goal of the desirability function was to decrease all emission responses. The plotted lines are the prediction lines of the independent variables. The vertical solid lines for each variable is the current factor setting. By changing the vertical solid line for each independent variable, the horizontal dashed lines were updated by re-computing the predicted response at the new factor setting. The horizontal dashed lines show the final predicted response according to the factor settings.

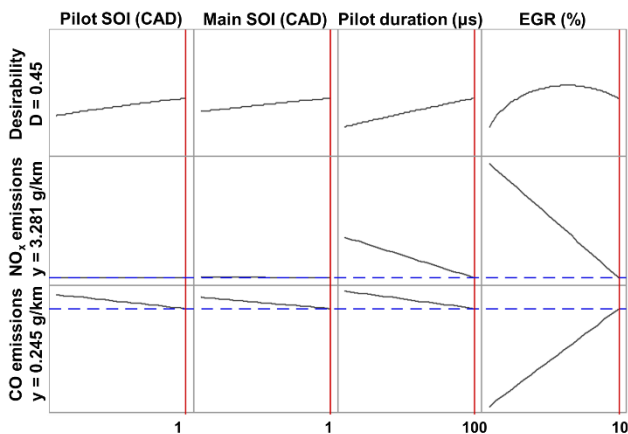


Figure 6. Desirability plot for the first factorial design.

Pilot injection SOI, main injection SOI and pilot injection duration all resulted in emission reduction for the high parameter values (Table 5). EGR has a maximum desirability value approximately in the middle of the low and high EGR values. This is because of the reduction in NO_x emissions and the increase in CO emissions for increasing values of EGR.

For the second factorial design, all the high values of the engine parameters were chosen. This resulted in a

desirability factor of $D=0.45$, which as seen in Figure 6. However, this is not the maximum achievable desirability value. This compromise is acceptable because the increase in CO emissions is still under the EU legislated limit of 0.5 g/km, therefore extra 'weighting' was given to the reduction of NO_x. Retarding the pilot SOI and the main SOI contributed to a decrease in CO emissions. The increase of the pilot injection duration with 100 µs contributes to the decrease in both CO emissions and NO_x emissions. The low and high values for the second factorial design are listed in Table 6. The differences between the second factorial design's parameters have been increased by 50 % except for the pilot injection duration. This smaller increase in the difference between the low and high value of the pilot injection duration was to limit the possibility of an overlap in the pilot fuel injection and main fuel injection during the simulation.

Table 6. Independent variables and their levels for the second factorial design.

Independent variables	Variable levels		
	Low	High	Δ
EGR (%)	10	25	15
Pilot injection SOI (CAD)	1	4	3
Pilot injection duration (µs)	100	200	100
Main injection SOI (CAD)	1	4	3

SECOND FACTORIAL DESIGN

For the second factorial design, again EGR percentage has the greatest effect on both CO emissions and NO_x emissions. Similarly to the first factorial design, the change in main injection SOI and pilot injection SOI have a negligible effect on engine emissions and pilot duration causes a small decrease in CO emissions. The desirability function for the second factorial design was set to minimise NO_x emissions as well as reach a CO emissions target of 0.5 g/km (based on Euro Standards). A desirability factor of $D=0.33$ was achieved with the CO emissions target of 0.5 g/km, but not being able to also minimise NO_x emissions to the lowest possible value.

Table 7. Independent variables and their levels for the third factorial design.

Independent variables	Variable levels		
	Low	High	Δ
EGR (%)	25	47.5	22.5
Pilot injection SOI (CAD)	1	4	3
Pilot injection duration (µs)	200	300	100
Main injection SOI (CAD)	1	4	3

For the third factorial design, the low and high values for the independent values were chosen as listed in Table 7. The increase in EGR percentage was chosen to further investigate its effect on achieving LTC, even though it will result in CO emissions increasing above the EU's legislated limit of 0.5 g/km. Changes in pilot

injection SOI and main injection SOI were kept to the same values as the second factorial design. Pilot injection duration was increased as after the EGR percentage, pilot injection duration also decreases CO emissions.

THIRD FACTORIAL DESIGN

Main effect plots are shown in Figure 7 and Figure 8 for CO emissions and NO_x emissions for the third factorial design. EGR percentage has the greatest effect on both CO emissions and NO_x emissions. The desirability plot for the third factorial design, shown in Figure 9, was set to minimise CO emissions and NO_x emissions. A desirability factor of $D = 0.15$ was achieved by maximising the EGR percentage to get the lowest possible NO_x emissions. This resulted in an increase of CO emissions, which negatively affected the desirability factor.

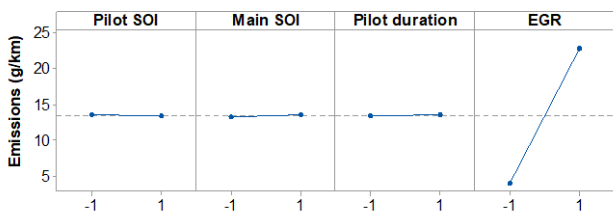


Figure 7. Variation of CO emissions against high and low levels for each of the main effects, for the third factorial design.

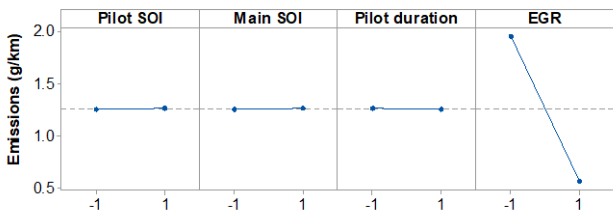


Figure 8. Variation of NO_x emissions against high and low levels for each of the main effects, for the third factorial design.

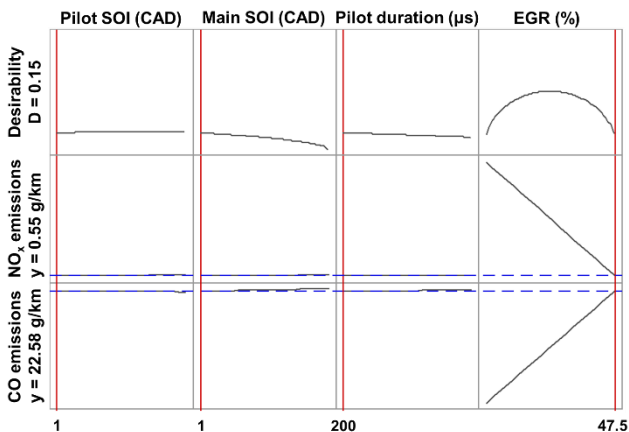


Figure 9. Desirability plot for the third factorial design.

For all factorial designs considered, the interaction effects between the four parameters investigated were not significant ($p > 0.02$) and was omitted from the results discussion.

Figure 10 and Figure 11 considered the engine's response for the selection of the engine parameters for each factorial design and compared it to emission results from an engine that does not operate with pilot injections or EGR. On both figures, the Euro 4 emission limit is indicated in a horizontal line. The results from the second factorial design were able to achieve a reduction of NO_x emissions of approximately 18 % by introducing an EGR percentage of 12 %, increasing the pilot duration by 200 μ s and retarding both the main injection SOI and the pilot injection SOI by 1 CAD. CO emissions were kept at the Euro 4 emission limit of 0.5 g/km. By increasing the EGR percentage to 47.5 %, the engine's NO_x emissions were reduced by approximately 86 %. However, CO emissions increased to 22.58 g/km because of the increase in EGR percentage.

Unlike greenhouse gases such as CO₂, the risks from NO_x are focused on in the locality and NO_x reduction in diesel exhaust has become a politically sensitive matter [30]. Intervention needs to be targeted to areas of NO_x emission sources. There is also evidence that compression ignition vehicles primarily contribute to NO_x emissions, compared to spark ignition vehicles [31]. The prioritisation to reduce NO_x emissions over CO emissions is also driven by the possible increase in capital and running costs for after treatment system to remove NO_x emissions from diesel exhaust [3].

Figure 12 shows the heat release of the engine at 2500 rpm and 25 % load when the engine is running without EGR and pilot injections (no LTC) as well as when the engine is running with the parameters as determined in the third factorial design. The start of combustion (SOC) becomes advanced compared to when the engine is running with no LTC. The advance in SOC is caused by the introduction of a pilot injection. Also, the increased amount of fuel delivered by the pilot injection contributes to the SOC advancing [32]. With an increase of the pilot injection duration of 200 μ s for the third factorial design, the percentage of the pilot injection has increased from 25 % to 50 % of the total mass injected.

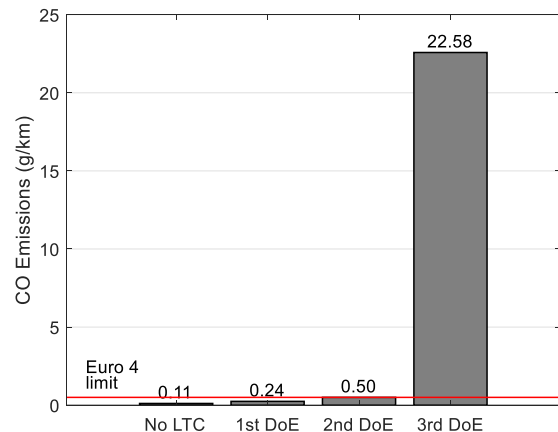


Figure 10. Simulated CO emissions of the engine when run over the WLTP for the different factorial designs.

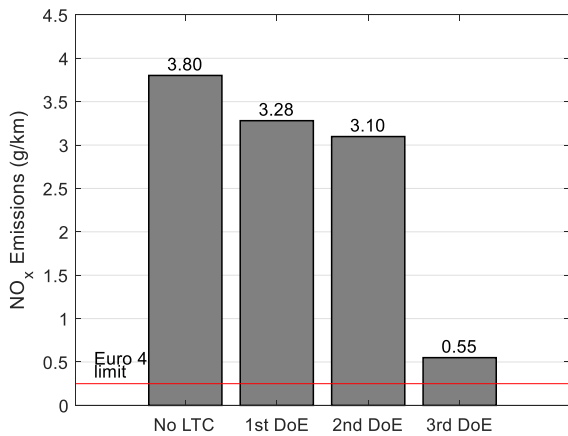


Figure 11. Simulated NO_x emissions of the engine when run over the WLTP for the different factorial designs.

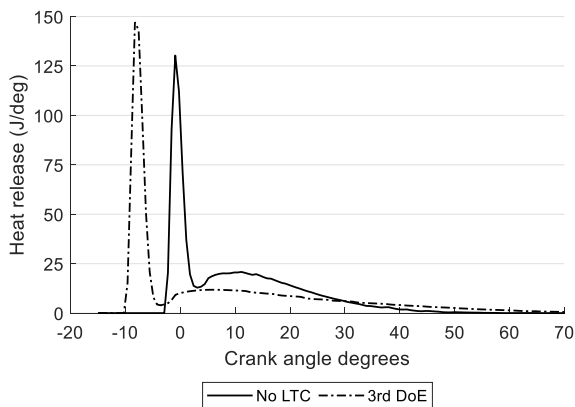


Figure 12. Simulated rate of heat release at 2500 rpm and 25 % load for different engine operating conditions.

The heat release diagram in Figure 12 for the third factorial design shows a significant drop in the heat released in the diffusion combustion phase with an increase in heat released in the premixed combustion phase compared to the heat release trace for an engine operating without LTC. The heat release during diffusion combustion is significant in the case of conventional diesel combustion and is much smaller or even absent in the case of LTC [3]. Figure 13 shows the cylinder temperature for the third factorial design as well as for when the engine is running without EGR and the use of pilot injections. There is a decrease in peak combustion temperature of approximately 100 °C when EGR and pilot injections are used compared to when it is not used. The period just after start of combustion where the combustion temperature is higher for the third DoE compared to the no LTC case, is caused by the increased fuel mass fraction burned in the premixed phase (Figure 12). The increased temperature during the intake and compression stages are due to the EGR increasing the charge temperature.

Engine operation with the use of the engine parameters determined by the third factorial design thus shows LTC characteristics that include increased mass fuel burned in the premixed burn phase as well as decreased peak combustion temperatures. It can be concluded that the engine is running in LTC conditions with an EGR percentage of 47.5 % and an

increase in the pilot injection duration of 300 μs. The use of LTC can assist in decreasing engine out emissions such as NO_x emissions. Extensive use of EGR can reduce NO_x emissions with approximately 85 % which will decrease the stress on after treatment systems for the removal of NO_x emissions. The increase of CO emissions as a result of the use of EGR can result in increased capabilities required from the diesel oxidation catalyst to remove the additional CO emissions from the exhaust stream. CO emissions can be reduced by improving the fuel mixing capabilities with the use of early pilot injections as well as increasing the amount of fuel delivered by the pilot injection. Engine manufacturers can use LTC to reduce NO_x emissions by approximately 18 % and still comply with the EU's CO emission limits, or optimise toward an optimum emissions reduction point with the use of LTC and after treatment systems that will reduce the total cost of after treatment systems and thus the overall cost to the consumer [3].

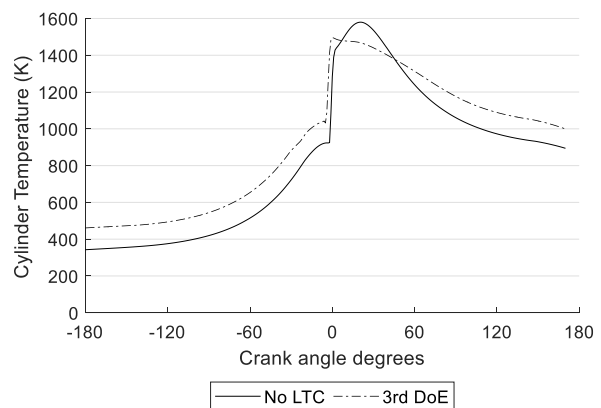


Figure 13. Simulated combustion temperature at 2500 rpm and 25 % load for different engine operating conditions.

CONCLUSION

This paper publishes a study of the use of DoE to reduce the emissions (CO, NO_x) from a simulated transient compression ignition engine running over the WLTP with LTC. The study was successful and the main conclusions are:

1. With the focus on minimising NO_x, a reduction of approximately 85% was achieved with EGR percentages of 47.5 %, retarding the pilot and main SOI by 1 CAD and increasing the pilot injection duration by 300 μs.
2. The CO-NO_x trade-off is still evident in LTC. NO_x emissions were reduced by approximately 18 % with the use of 12 % EGR without exceeding the Euro 4 CO emissions limit. A further increase in EGR percentage significantly increases the engine's CO emissions.
3. Low temperature combustion was achieved, as evidenced from analysis of the rate of heat release and combustion temperature.
4. Advancing the pilot injection SOI and increasing the pilot injection duration improves combustion and reduces CO emissions.

5. It is difficult to achieve an acceptable desirability factor when multiple engine responses need to be minimized. Sound judgement by the researcher is necessary to determine which response is more important.
6. The method of using DoE to minimise engine out emissions was successful.

LIMITATIONS

It should be noted that the methodology used in this study is a pilot study to examine the feasibility of using an engine and vehicle simulation together with DoE to determine transient emissions. This has been successful, but there are a number of limitations that prevent wider conclusions being drawn:

- The sample size of the experimental data used in this study to validate the engine combustion and emissions model is modest. Future studies will have a more comprehensive validation.
- A blind transient comparison between the results of the simulated DoE and an experimental DoE would increase the confidence in the results of the simulated model. This is planned for in the future.
- The method of determining the next factorial design's parameters by following the path of greatest emission reduction, was successful, but it can result in finding a local minimum, rather than the global minimum for emissions reduction. The DoE can be improved by investigating the whole operating map of the engine.

REFERENCES

1. European Union., "Regulation (EC) No 443/2009 of the European Parliament and of the Council of 23 April 2009 setting emission performance standards for new passenger cars as part of the Community's integrated approach to reduce CO₂ emissions from light-duty vehicles," OJ L140/1, 2009.
2. Musculus, M.P.B., Miles, P.C., and Pickett L.M., "Conceptual models for partially premixed low-temperature diesel combustion." *Progress in Energy and Combustion Science* 39(2-3): 246-283, 2013, doi: j.pecs.2012.09.001.
3. Dev, S., B Chaudhari, H., Gothekar, S., Juttu, S. et al., "Review on Advanced Low Temperature Combustion Approach for BS VI," SAE Technical Paper 2017-26-0042, 2017, doi:10.4271/2017-26-0042.
4. Asad, U., and Zheng, M., "Efficacy of EGR and Boost in Single-Injection Enabled Low Temperature Combustion," *SAE Int. J. Engines* 2(1):1085-1097, 2009, doi:10.4271/2009-01-1126.
5. Carlucci, P., Ficarella, A., and Laforgia, D., "Effects of Pilot Injection Parameters on Combustion for Common Rail Compression ignition engines," SAE Technical Paper 2003-01-0700, 2003, <https://doi.org/10.4271/2003-01-0700>.
6. Horibe, N. and Ishiyama, T., "Relations among NO_x, Pressure Rise Rate, HC and CO in LTC Operation of a Compression ignition engine," SAE Technical Paper 2009-01-1443, 2009, <https://doi.org/10.4271/2009-01-1443>.
7. Tuner, M., "Review and Benchmarking of Alternative Fuels in Conventional and Advanced Engine Concepts with Emphasis on Efficiency, CO₂, and Regulated Emissions," SAE Technical Paper 2016-01-0882, 2016, doi:10.4271/2016-01-0882.
8. Biswas, S., Bakshi, M., Shankar, G., and Mukhopadhyay, A., "Optimization of Multiple Injection Strategies to Improve BSFC Performance of a Common Rail Direct Injection Compression ignition engine," SAE Technical Paper 2016-28-0002, 2016, doi:10.4271/2016-28-0002.
9. Zhang, Q., Ogren, R., and Kong, S., "Trade-Offs Between Emissions and Efficiency for Multiple Injections of Neat Biodiesel in a Turbocharged Compression ignition engine Using an Enhanced PSO-GA Optimization Strategy," SAE Technical Paper 2016-01-0630, 2016, doi:10.4271/2016-01-0630.
10. Toshitaka M., Takeuchi K., and Shimazaki N., "Reduction of compression ignition engine NO_x using pilot injection." SAE Technical Paper 950611, 1995, doi: 10.4271/950611.
11. Akihama, K., Takatori, Y., Inagaki, K., Sasaki, S. et al., "Mechanism of the Smokeless Rich Diesel Combustion by Reducing Temperature," SAE Technical Paper 2001-01-0655, 2001, doi:10.4271/2001-01-0655.
12. Knight, B., Bittle, J., and Jacobs, T., "Characterizing the Influence of EGR and Fuel Pressure on the Emissions in Low Temperature Diesel Combustion," SAE Technical Paper 2011-01-1354, 2011, doi:[10.4271/2011-01-1354](https://doi.org/10.4271/2011-01-1354).
13. Yao, M., Zhang, Q., Liu, H., Zheng, Z. et al., "Compression ignition engine Combustion Control: Medium or Heavy EGR?" SAE Technical Paper 2010-01-1125, 2010, doi:[10.4271/2010-01-1125](https://doi.org/10.4271/2010-01-1125).
14. Abu-Jrai A, Yamin JA, Alaa H et al. Combustion characteristics and engine emissions of a diesel engine fueled with diesel and treated waste cooking oil blends. *Chemical Engineering Journal* 172(1): 129-136, 2011.
15. Zheg M, Mulenga MC, Reader GT et al. Influence of biodiesel fuel on diesel engine performance and emissions in low temperature combustion. Technical report, SAE Technical Paper, 2006.
16. Gaballo, M., Giodice, M., Diano, A., Fersini, F. et al., "Application of a Modular Simulation Approach: Optimizations from Combustion to Vehicle Management," SAE Technical Paper 2015-24-2505, 2015, doi:10.4271/2015-24-2505.

17. Minitab Inc., "Minitab Help File," 2010, www.minitab.com.
18. Montgomery, C., "Design and Analysis of Experiments," John Wiley & Sons, 2017.
19. Pandian, M., Sivapirakasam, S.P., and Udayakumar, M., "Investigation on the effect of injection system parameters on performance and emission characteristics of a twin cylinder compression direct injection engine fuelled with pongamia biodiesel–diesel blend using response surface methodology," *Applied Energy* 88(8): 2663-2676, 2017, doi: 10.1016/j.apenergy.2011.01.069.
20. Win, Z., Gakkhar, R.P., Jain, S.C., and Bhattacharya, M. "Investigation of compression ignition engine operating and injection system parameters for low noise, emissions, and fuel consumption using Taguchi methods," *Proceedings of the Institution of Mechanical Engineers, Part D: Journal of Automobile Engineering* 219(10): 1237-1251, 2005, doi: 10.1243/095440705X34865.
21. Ganapathy, T., Murugesan, K., and Gakkhar, R.P., "Performance optimization of Jatropa biocompression ignition engine model using Taguchi approach." *Applied Energy* 86(11): 2476-2486, 2009, doi: 10.1016/j.apenergy.2009.02.008.
22. Van Niekerk, A.S., Kay, P.J., Drew, B., and Larsen, N., "Development of multi-fidelity powertrain simulation for future legislation," presented at IMechE Internal Combustion Engines, UK, December 6-7, 2017.
23. Department for Transport, "Statistical data set: Cars (VEH02)," <https://www.gov.uk/government/statistical-data-sets/veh02-licensed-cars>, accessed November 2018.
24. d'Ambrosio, S. and Ferrari, A., "Potential of multiple injection strategies implementing the after shot and optimized with the design of experiments procedure to improve compression ignition engine emissions and performance." *Applied Energy* 155, 933-946, 2015, doi: 10.1016/j.apenergy.2015.05.124.
25. Spessa, E., D'Ambrosio, S., Iemmolo, D., Mancarella, A. et al., "Steady-State and Transient Operations of a Euro VI 3.0L HD Compression ignition engine with Innovative Model-Based and Pressure-Based Combustion Control Techniques," *SAE Int. J. Engines* 10(3):1080-1092, 2017, doi: 10.4271/2017-01-0695.
26. d'Ambrosio, S. and Ferrari, A., "Effects of exhaust gas recirculation in compression ignition engines featuring late PCCI type combustion strategies." *Energy Conversion and Management* 105, 1269-1280. 2015, doi: 10.1016/j.enconman.2015.08.001.
27. Posada F., Chambliss S., and Blumberg K., "Cost of emission reduction technologies for heavy duty vehicles" International Council for Clean Transportation, Feb 2016.
28. Piano, A., Millo, F., Boccardo, G., Rafigh, M. et al., "Assessment of the Predictive Capabilities of a Combustion Model for a Modern Common Rail Automotive Compression ignition engine," SAE Technical Paper 2016-01-0547, 2016, doi:10.4271/2016-01-0547.
29. Ravikumar, K., Krishnan, S., Ramalingam, S., and Balu K. "Optimization of process variables by the application of response surface methodology for dye removal using a novel adsorbent," *Dyes and Pigments* 72:66-74, 2007, doi: 10.1016/j.dyepig.2005.07.018.
30. Department for Environment Food & Rural Affairs, "UK plan for tackling roadside nitrogen dioxide concentrations," www.gov.uk/government/publications, accessed June 2018.
31. Air Quality Expert Group, "Nitrogen Dioxide in the United Kingdom," www.airquality.co.uk, Accessed June 2018.
32. de Ojeda, W., Zoldak, P., Espinosa, R., and Kumar, R., "Development of a fuel injection strategy for diesel LTC," SAE Technical Paper 2008-01-0057, 2008, doi: 10.4271/2008-01-0057.
33. Newhall, H.K., "Kinetics of engine-generated nitrogen oxides and carbon monoxide," *Symposium (International) on Combustion*, 12(1):603-613, 1969, doi:10.1016/S0082-0784(69)80441-8.
34. Fenimore, C.P., "Formation of nitric oxide in premixed hydrocarbon flames," *Symposium (International) on Combustion*, 13(1):373-380, 1971, doi: 10.1016/S0082-0784(71)80040-1.
35. Heywood, J.B., "Internal Combustion Engine Fundamentals," New York: McGraw-Hill, Inc., 1988.

CONTACT

Adriaan van Niekerk

Email: adriaan.vanniekerk@uwe.ac.uk

DEFINITIONS, ACRONYMS, ABBREVIATIONS

aTDC: after Top Dead Center

CAD: Crank angle degree

DoE: Design of Experiment

ECU: Engine control unit

EGR: Exhaust gas recirculation

EU: European Union

LTC: Low Temperature Combustion

MI: Main injection

NEDC: New European Drive Cycle

PI: Pilot injection

SOC: Start of combustion

SOI: Start of injection

TDC: Top dead center

WLTP: Worldwide Harmonised Light-duty Vehicles Test Procedures

APPENDIX

In order to ensure that the base simulation that was used to optimise the engine response is accurate, the simulation needed to be validated against experimental data. A total of nine experimental points at engine loads of 25 %, 50 % and 75 % at engine speeds of 2000 rpm, 2500 rpm and 3000 rpm were used in the validation process. Properties of the reference diesel used in the experimental tests are listed in Table 8.

Table 8: Properties of fuel used in experimental tests.

Fuel property	Value
Cetane number	51.7
LHV (MJ/kg)	42.8
Density @ 15°C (kg/m ³)	831.1
Viscosity @ 40°C (mm ² /s)	2.686
Oxygen content (%)	0

Output in the form of emissions data as well as in-cylinder pressure profiles were generated and used to validate the simulation's emission and combustion models.

CO EMISSIONS MODEL

For the calculation of CO emissions the software uses the concentration ratio of CO and CO₂ for the fuel concentration:

$$\frac{[\text{CO}]}{[\text{CO}_2]} = \max\left(\frac{1}{\sqrt{K_{pW}}}, \frac{1}{K_{pN}} \frac{[\text{H}]}{[\text{OH}]}\right) \quad (5)$$

where K_{pN} is the equilibrium constant of the reaction as suggested by Newhall [33] and K_{pW} is the equilibrium constant of the reaction as used by the software's gas property calculations.

The validation of the simulated CO emissions of the engine simulation compared to steady-state experimental results at 50 % engine load are shown in Figure 14. Simulated results are in good agreement with the experimental values.

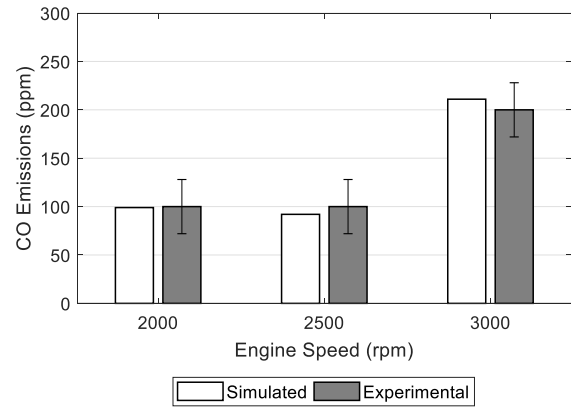


Figure 14: CO engine emissions comparison for different engine speeds at 50 % load.

NO_x EMISSIONS MODEL

The software's NO_x emissions model accounts for the formation of prompt NO from the correlation data as reported by Fenimore [34] which gives the ratio of prompt NO to equilibrium NO as a function of equivalence ratio. The thermal NO formation is described by the Zeldovich mechanism below:



The concentration of NO versus time is solved using an open system in which Equation 6 is used with the rate constants reported by Heywood [35] The first reaction equation, R_1 , is given by:

$$R_1 = A \cdot \text{ARC}_1 e^{T_a \cdot \text{AERC}_1 / T} \quad (7)$$

For the second and third reaction equations, the rate constant $R_{2/3}$, is given by:

$$R_{2/3} = A \cdot e^{T_a / T} \quad (8)$$

where A is the pre-exponential constant, ARC_1 is the user defined pre-exponent multiplier, AERC_1 is the user defined exponent multiplier, T is the burned zone temperature and T_a is the activation temperature for the reaction. Values for ARC_1 are kept at 1.5 for all cases and the values of AERC_1 are shown in Table 9.

The validation of the simulated NO_x emissions of the engine simulation compared to steady-state experimental results are shown in Figure 15. The emissions model was calibrated against the experimental values using the user-defined values in Equation 7. Simulated results are in good agreement with the experimental values.

Table 9: User defined values for AERC₁ for the NO_x emission sub-model

Engine load (%)	AERC ₁
	2000 rpm
25	0.95062
50	1.12603
75	1.06222
	2500 rpm
25	0.90000
50	1.12222
75	1.11667
	3000 rpm
25	1.21667
50	1.11070
75	1.07592

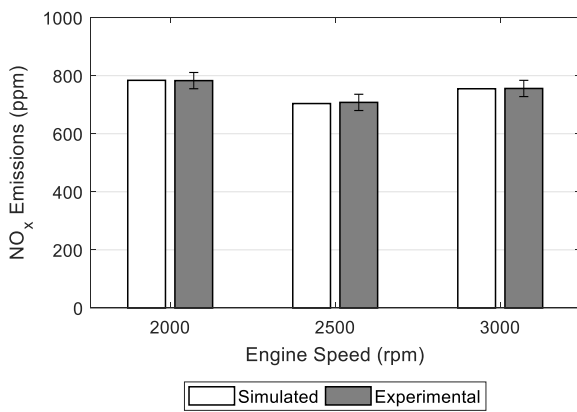


Figure 15: NO_x engine emissions comparison for different engine speeds at 50% load.

SIMULATED COMBUSTION MODEL

Experimental in-cylinder pressure profiles from previous published work [22] are available for the test engine at different engine speeds and load percentages. Table 10 shows the statistical analysis of the experimental in-cylinder pressure data that was used in the combustion model validation process.

Table 10: Statistical analysis of the maximum measured in-cylinder pressure.

Engine load (%)	n	Mean (bar)	StDev (bar)
		2000 rpm	
25	16	65.5	± 3.3
50	28	80.0	± 0.9
75	15	133.7	± 6.4
		2500 rpm	
25	48	65.8	± 1.9
50	40	84.1	± 1.6
75	48	132.6	± 1.6
		3000 rpm	
25	40	58.9	± 1.3
50	38	81.6	± 0.9
75	41	109.3	± 2.2

From the pressure profiles, the simulation can calculate the heat release profile and generate a fuel mass burn profile that can be used in the simulation's combustion calculations. The calculated mass in the fuel mass burn profile is used to generate a multi-component Wiebe combustion model to account for premixed, diffusion and tail combustion:

$$W_n = 1 - \exp[-a(\theta_i - \theta_0)^{m+1}] \quad (9)$$

where W_n is the non-dimensional cumulative mass fraction burned, a represents the combustion efficiency and has been fixed to 6.9 so that 99.9% of fuel is burnt at the end of combustion, m is the Wiebe exponent, θ_i is the i_{th} crank angle and θ_0 is the start of combustion crank angle. When the burn rate curve consists of more than one Wiebe function, the overall cumulative burn profile is:

$$W = \sum_n f_n \cdot W_n \quad (10)$$

where f_n is the mass fraction burned for each individual Wiebe function. For the experimental mass burn profile, two Wiebe functions were selected to characterise the premixed and diffusion burn profile of the experimental results.

A correlation analysis has been carried out to derive multiple regression equations that express the parameters as a function of engine operating values. The developed correlations are as follows:

$$\theta_0 = 24.95 - 6.93p_0 + 0.689\theta_{minj} \quad (11)$$

where p_0 is the inlet charge pressure in bar and θ_{minj} is the injection timing of the main fuel injection in degrees after Top Dead Center (aTDC).

$$f_n = -3.55 - 0.0524\theta_{pinj} + 0.007056\Delta\theta_{pinj} \quad (12)$$

where θ_{pinj} is the injection timing of the pilot fuel injection in degrees aTDC and $\Delta\theta_{pinj}$ is the injection duration of the pilot injection in microseconds.

$$m_p = 1.027 - 0.000240N \quad (13)$$

$$m_d = 1.027 - 0.0002N \quad (14)$$

where N is the engine speed in revolutions per minute (rpm). All the terms of the correlation equations generated for the Wiebe combustion model were found to be significant with $p < 0.02$. Furthermore, the regression statistics goodness of fit (R^2) showed high values of 93% for θ_0 , 97% for f_n , 65% for m_p and 71% for m_d .

Figure 16, Figure 17 and Figure 18 show the comparison between the experimental in-cylinder pressure profile and the simulated result when using the multi-Wiebe combustion model.

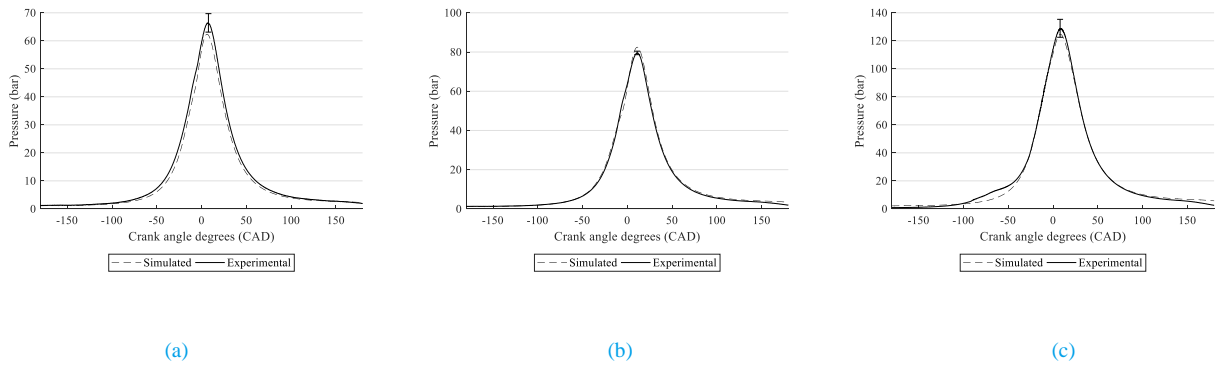


Figure 16: In-cylinder pressure profile comparison between steady-state experimental data and simulated data at 2000 rpm for (a) 25 % load, (b) 50 % load and (c) 75 % load.

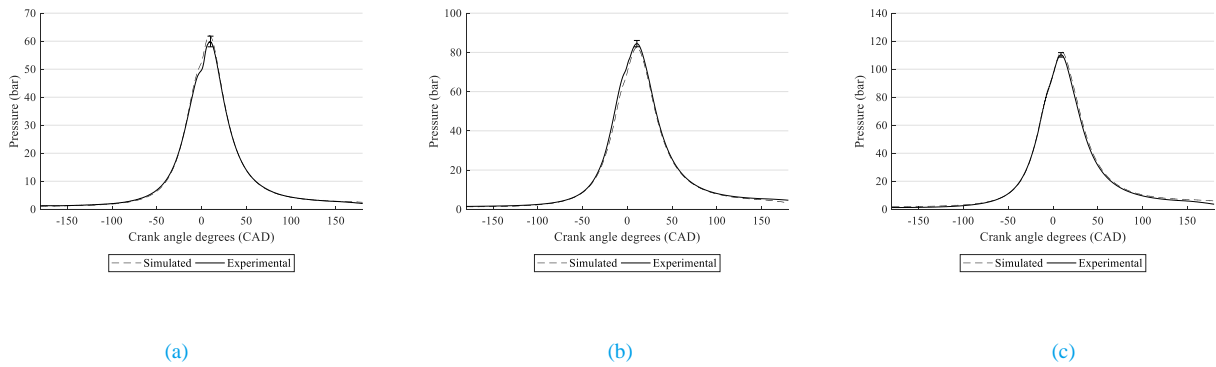


Figure 17: In-cylinder pressure profile comparison between steady-state experimental data and simulated data at 2500 rpm for (a) 25 % load, (b) 50 % load and (c) 75 % load.

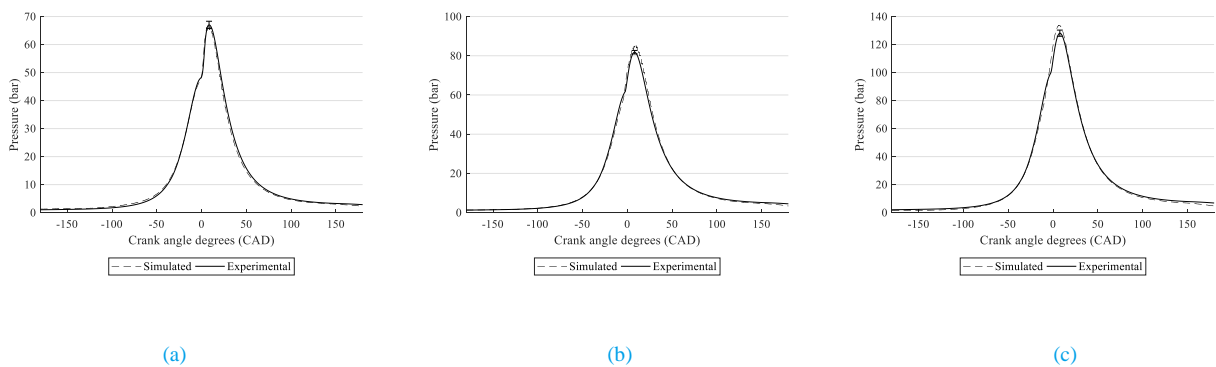


Figure 18: In-cylinder pressure profile comparison between steady-state experimental data and simulated data at 3000 rpm for (a) 25 % load, (b) 50 % load and (c) 75 % load.

